High-Resolution One-Way Reflection Waveform Inversion

Abolhassani, S.; Verschuur, E.

Important note
To cite this publication, please use the final published version (if applicable).
Please check the document version above.

High-Resolution One-Way Reflection Waveform Inversion

S. Abolhassani[1], E. Verschuur[1]

[1] Delft University of Technology

Summary

Reflection waveform inversion (RWI) is a method that relies on primary pure reflection data to recover the subsurface background velocity based on the associated evolving seismic images. Background velocity updates estimated by conventional RWI are nonoptimal, which is partly attributed to low-resolution tomographic wavepaths and migration isochrones. Preconditioning RWI sensitivity kernels using Hessian information solves this problem but is not practical for a large number of model parameters. One-way reflection waveform inversion (ORWI) is a reflection waveform tomography technique in which the forward modeling scheme operates in one direction (downward and then upward) via virtual parallel data levels in the medium. The ORWI framework allows us to break down the Hessian matrix into smaller operators, which makes the preconditioning operation more efficient and less computationally expensive. This extended abstract turns conventional ORWI into a high-resolution but computationally feasible ORWI (Gauss-Newton ORWI) to improve the nonoptimal background velocity updates.

High-Resolution One-Way Reflection Waveform Inversion

Introduction

While conventional full waveform inversion (FWI) (Tarantola, 1984) has been widely used to estimate subsurface properties for shallow targets, relying on refractions and diving waves, and has been shown to be a powerful tool for this purpose, it may not be able to accurately estimate deep targets using only refractions and diving waves that are observed on the relatively limited-offset acquisition lines. This can make achieving optimal results challenging for deep targets using FWI (e.g., Brittan and Jones, 2019). Reflection Waveform Inversion (RWI) was born (e.g., Xu et al., 2012) to sample deep targets using pure reflection data. Conventional RWI is a reflection waveform tomography technique that maps an evolving stacked image in every cycle (Figure 1) to reconstruct the subsurface background velocity model based on that. Conventional RWI alternatingly solves a two-parameter—background velocity and reflectivity—minimization problem.
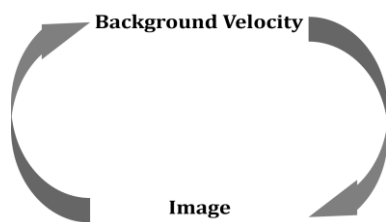

Figure 1 *Conventional RWI cycle in which background velocity and image reconstructions alternate.*
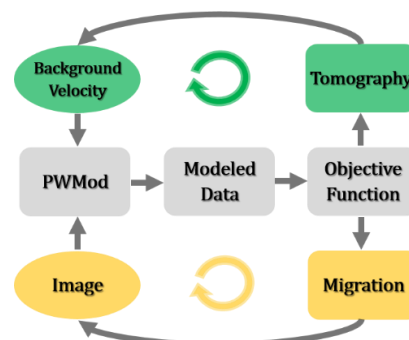

Figure 2 *ORWI cycle uses one-way primary wavefield modeling (PWMod) and alternates between background velocity and image reconstructions via the same objective function.*

Berkhout (2012) introduced joint migration inversion (JMI), an RWI technique based on a one-way wavefield decomposition scheme. JMI uses a forward modeling scheme called full-wavefield modeling (FWMod) to model full (both primaries and multiples) downgoing and upgoing reflection wavefields. This means that the full wavefield is modeled in only one direction (downward and then upward).

With the same idea as JMI for reflection waveform inversion, but after limiting FWMod to primary wavefield modeling (PWMod), no multiples and transmission effects, we introduce one-way reflection waveform inversion (ORWI). Figure 2 shows the ORWI cycle. Due to proper parameterization in PWMod, the sensitivity kernels for migration (isochrones) and tomography (rabbit-ears) are isolated in ORWI. As a result, the migration and tomography sensitivity kernels can be calculated independently, freeing tomograms from high local model wavenumbers. ORWI is also computationally cheaper than its alternatives that use the finite-difference method for forward and adjoint wavefield modeling.

Nonoptimal background velocity updates in RWI are partly linked to low-resolution seismic images with unpreserved amplitudes (Gomes and Yang, 2018). The same reasoning can also be used to attribute the poor background velocity updates of RWI to low-resolution tomographic wavepaths. Pratt et al. (1998) showed that the Gauss-Newton optimization method in waveform inversion reconstructs accurate velocity updates with higher resolution in every iteration than the gradient-based methods since it uses the second-order derivatives of the objective function (Hessian information) to precondition the gradient. However, due to the computation of the Hessian matrix, the Gauss-Newton method for large-scale seismic problems requires more memory and time, making it prohibitively costly. There have been multiple attempts so far to approximate a proper but cheaper preconditioner (e.g., Jun et al., 2015; Lu et al., 2018). Recently, Abolhassani and Verschuur (2022a) proposed a cheap, depth-based, data-domain preconditioner in the context of iterative least-squares one-way wave-equation migration (LS-WEM) for image reconstruction. This expanded abstract will build on their proposal for a cheap, depth-based preconditioner for high-resolution background velocity reconstruction with ORWI.

One-Way Reflection Waveform Inversion (ORWI)

ORWI is a technique used to reconstruct the subsurface velocity structure of a medium based on a primary wavefield modeling scheme, known as PWMod, working based on the Kirchhoff-integral for a loss-free homogenous medium for parallel data surfaces (Berkhout, 1982). For virtual parallel data levels, PWMod in the space-frequency domain reads the following equation to model the two-way surface seismic reflection data recursively in-depth,

$$\mathbf{p}_{\text{mod}}^-(z_0) = \sum_{m=N}^{1} \mathbf{W}_{z_0:z_m}^- \left(\mathbf{r}^\cup(z_m) \circ \overbrace{\mathbf{W}_{z_m;z_0}^+ \mathbf{s}^+(z_0)}^{\mathbf{P}_{\text{mod}}^+(z_m)} \right), \tag{1}$$

where $\mathbf{p}_{\text{mod}}^-(z_0)$ and $\mathbf{p}_{\text{mod}}^+(z_m)$ are the monochromatic upgoing wavefield received at the depth level z_0 and the downgoing wavefield received at the depth level z_m, respectively, $\mathbf{W}_{z_w:z_0}^+$ is the monochromatic total downward propagation operator and contains the matrix multiplication of all the downward propagation operators required to reach from z_0 to z_m, $\mathbf{W}_{z_0:z_m}^-$ is the monochromatic total upward propagation operator and contains the matrix multiplication of all the upward propagation operators required to reach from z_m to z_0, $\mathbf{r}^\cup(z_m)$ represents the angle-independent upward reflectivity operator at z_m, $\mathbf{s}^+(z_0)$ indicates the downgoing monochromatic physical source at the Earth's surface (z_0), N denotes the number of parallel data depth levels, and the symbol $\circ$ shows the point-wise product between the vectors.

Expanding $p_{\text{mod}}^+(x_A, z_{m+1}, \omega_\kappa)$ reads (Berkhout, 1982):

$$p^+(x_A, z_{m+1}, \omega_\kappa) = \frac{1}{2\pi} \int_{-\infty}^{+\infty} p^+(x, z_m, \omega_\kappa) \left(\overbrace{\int_{-\infty}^{+\infty} e^{+\iota \sqrt{\left(\frac{\omega_\kappa}{c_A}\right)^2 - k_x^2} |z_{m+1} - z_m|} e^{-\iota k_x (x_A - x)} dk_x}^{\text{downward propagation kernel: } w_{z_{m+1};zm}^+} \right) dx, \tag{2}$$

in which the downward propagation kernel is marked, A denotes the lateral location on z_{m+1}, ω_κ shows an angular frequency component, c is the acoustic phase velocity, and $|z_{m+1} - z_m|$ is the extrapolation step. PWMod assumes that the medium is vertically homogeneous within an extrapolation step, so the extrapolation steps must be small enough. The propagation operator for lateral heterogeneous fluids must be modified to a space-variant convolutional operator (see Berkhout (1982) for details).

ORWI minimizes a two-parameter—background velocity and angle-independent upward reflectivity—objective function alternatingly for each class of parameters. For one shot and one angular frequency component, the objective function is simply defined as,

$$S(\mathbf{m}) = \frac{1}{2} \|\mathbf{p}_{\text{obs}}^-(z_0) - \mathbf{p}_{\text{mod}}^-(\mathbf{m}, z_0)\|_2^2, \tag{3}$$

where $\mathbf{m}$ denotes the model parameter vector and equals $\begin{pmatrix} \mathbf{r}^\cup \\ \mathbf{c} \end{pmatrix}$, $\mathbf{p}_{\text{obs}}^-(z_0)$ and $\mathbf{p}_{\text{mod}}^-(\mathbf{m}, z_0)$ are the observed and modeled primary reflection data at z_0, respectively.

High-Resolution Updates for ORWI

The Gauss-Newton model update equation for every cycle of ORWI takes the form of,

$$\Delta \mathbf{m}^{cycle} = \begin{bmatrix} \Delta \mathbf{r}^\cup \\ \Delta \mathbf{c} \end{bmatrix}^{cycle} = - \begin{bmatrix} \mathbf{H}_{\mathbf{r}^\cup}^{-1} & \mathbf{0} \\ \mathbf{0} & \mathbf{H}_{\mathbf{c}}^{-1} \end{bmatrix}^{cycle} \begin{bmatrix} \mathbf{g}_{\mathbf{r}^\cup} \\ \mathbf{g}_{\mathbf{c}} \end{bmatrix}^{cycle}, \tag{4}$$

in which $\mathbf{g}_{\mathbf{r}^\cup}$ is the imaging gradient, $\mathbf{g}_{\mathbf{c}}$ is the tomographic gradient, $\mathbf{H}$ is the Gauss-Newton Hessian approximation, and reads $\mathbf{H} = \text{Re}[\mathbf{J}^T \mathbf{J}^*]$, $\mathbf{J}$ is the partial derivative wavefield matrix (Jacobian) of the dimension: number of data points × number of model parameters, and $\mathbf{H}^{-1}$ acts as a pre-conditioner on the gradient direction to correctly update the model parameter update vector $\Delta \mathbf{m}$ in every cycle. Sun et al., (2019) provide more information on the gradient vector calculations. They show how PWMod helps the depth-by-depth calculation of the gradient vectors.

In the context of LS-WEM, Abolhassani and Verschuur (2022a) derived the Jacobian matrix for $\mathbf{r}^{\cup}$, the key term of Equation (4) for a solution. By similarity, we below derive the other key element of Equation (4), i.e., the ℓth column of the Jacobian matrix associated with c_ℓ at the given depth level z_m,

$$\frac{\partial \mathbf{p}_{\text{mod}}^-(z_0)}{\partial c_\ell(z_m)} = \left\{ \frac{\partial \mathbf{W}_{z_0;z_m}^-}{\partial c_\ell(z_m)} \mathbf{r}^{\cup}(z_m) \circ \mathbf{p}_{\text{mod}}^+(z_m) \right\} + \left\{ \frac{\partial \mathbf{W}_{z_m;z_0}^+}{\partial c_\ell(z_m)} \circ \mathbf{p}_{\text{mod}}^-(z_m) \right\}. \quad (5)$$

According to Equation (5), PWMod allows us to build the Jacobian matrix depth-by-depth, just as Abolhassani and Verschuur (2022a) derived the Jacobian matrix for $\mathbf{r}^{\cup}$. This feature decomposes the Hessian matrix into smaller operators (N operators with the dimension of data points × data points for every depth level) and greatly improves the computational efficiency of the Gauss-Newton inversion process. Indeed, by breaking the Hessian operator down into minimal operators that only operate on the partial derivative wavefields associated with a single depth level, we can make the Hessian computation feasible for large-scale problems.

Figure 3 compares the stacked image and one-source-receiver-pair tomogram corresponding to a flat reflector medium with a homogenous overburden after one cycle (1x migration and 1x tomography) of high-resolution ORWI (Gauss-Newton ORWI) and conventional ORWI (steepest-decent ORWI). It confirms the effectiveness of the Hessian inverse matrices applied to the imaging and tomographic gradients. As expected, the image deconvolution and tomogram deconvolution are clearly visible.
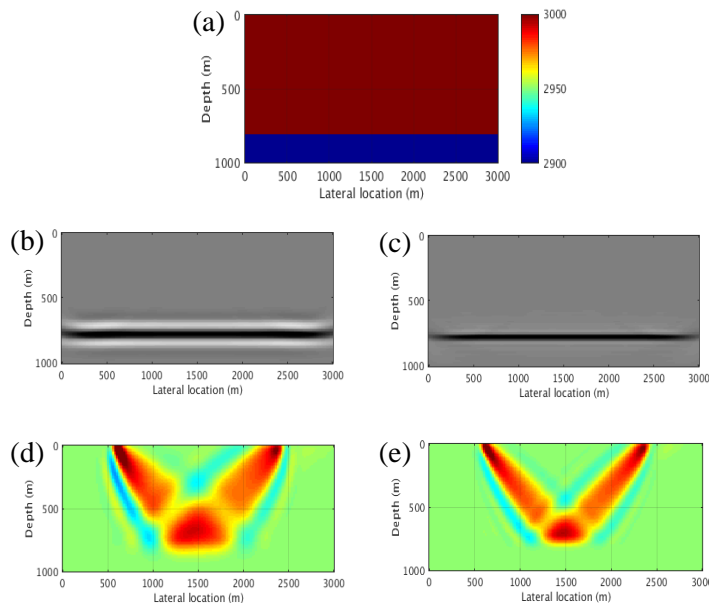

Figure 3 *Flat reflector example: Comparison between conventional ORWI (steepest descent) and high-resolution ORWI (Gauss-Newton). (a) True acoustic velocity model. (b) Estimated stacked image by conventional ORWI. (c) Estimated stacked image by high-resolution ORWI. (d) Estimated tomogram for a pair of source and receiver by conventional ORWI. (e) Estimated tomogram for a pair of source and receiver by high-resolution ORWI. Note that an initial velocity of 2900 m/s, an initial zero reflectivity model, and a maximum offset of 2000 m is used in this example.*

Numerical Experiment

To test high-resolution ORWI, We use it to invert for a faulted layered velocity model (Figure 4-a). The observed data is generated with a 10 Hz Ricker wavelet, a maximum offset of 4000 m, recorded for 2.04 s, and includes only primary reflections. The initial velocity model is a 1D linearly increasing gradient model (Figure 4-b), and the initial reflectivity is zero. The models are discretized with 201 grid points in the horizontal direction (20 m interval) and 166 grid points in the vertical direction (10 m interval). 41 shots with 100 m spacing are used, and each shot is recorded by 201 receivers. The full frequency band is inverted at once. Figure 4-c demonstrates the estimated tomogram using high-resolution ORWI after 40 cycles (each cycle includes 1x high-resolution migration and 1x high-resolution tomography). To address the reflectivity imprints on tomograms due to unfocused stacked images in early cycles, we follow Abolhassani and Verschuur (2022b). Figure 4-c confirms that the proposed high-resolution ORWI is effective. As seen, although we start with a 1D linearly increasing gradient background velocity model and invert the full frequency band (0-30 Hz) simultaneously, the missing layers from the background velocity model are properly recovered, and even the vertical fault is illuminated clearly.
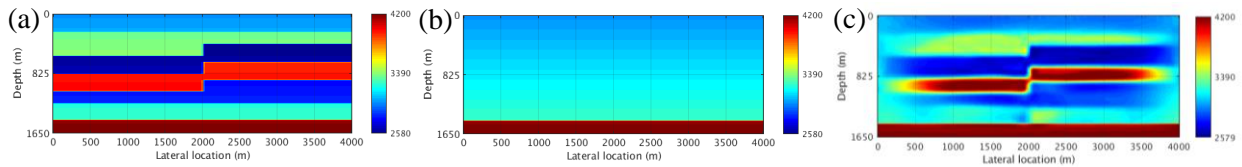
Figure 4 *Faulted layered medium example. (a) True velocity model. (b) Initial velocity model (1D initial gradient model). (c) Estimated tomogram by high-resolution ORWI after 40 cycles.*

Conclusions

Low-resolution images and tomographic wavepaths in RWI can result in nonoptimal tomographic updates. To address this issue, we introduced a Gauss-Newton one-way RWI technique (GN-ORWI) in which the Hessian matrix is calculated in a depth-marching regime, reducing the number of model parameters each time the Hessian and its inverse is calculated or stored. As a result, the Hessian computation in GN-ORWI becomes sensible and feasible compared to its alternatives. Through a flat reflector medium example, we verified the high-resolution nature of imaging and tomographic gradients in GN-ORWI in comparison to conventional ORWI. For a faulted layered medium, we verified how the cumulative high-resolution updates for ORWI leads to a superior final tomogram.

Acknowledgments

References

Abolhassani, S., & Verschuur, E. [2022a]. Towards a more robust joint migration inversion. EAGE Annual Conference & Exhibition, 1-5.

Abolhassani, S., & Verschuur, E. [2022b]. Fast Gauss-Newton full-wavefield migration. SEG/AAPG International Meeting for Applied Geoscience & Energy, Expanded Abstract, 2709-2713.

Berkhout, A. J. [1982]. Seismic migration, imaging of acoustic energy by wave field extrapolation, A Theoretical aspects. *Elsevier*.

Berkhout A. J. [2012]. Combining full wavefield migration and full waveform inversion, a glance into the future of seismic imaging. *Geophysics*, **77**(2), S43-S50.

Brittan, J., & Jones, I. [2019]. FWI evolution—From a monolith to a toolkit. *The Leading Edge*, **38**(3), 179-184.

Gomes, A., & Yang, Z. [2018]. Improving reflection FWI reflectivity using LSRTM in the curvelet domain. SEG International Exposition and Annual Meeting, Expanded Abstract, 1248-1252.

Jun, H., Park, E., & Shin, C. [2015]. Weighted pseudo-Hessian for frequency-domain elastic full waveform inversion. *Journal of Applied Geophysics*, 123, 1-17.

Lu, S., Liu, F., Chemingui, N., Valenciano, A., & Long, A. [2018]. Least-squares full-wavefield migration. *The Leading Edge*, **37**(1), 46-51.

Sun, Y., Verschuur, E., & Qu, S. [2019]. Research note: derivations of gradients in angle-independent joint migration inversion. *Geophysical Prospecting*, **67**(3), 572-579.

Tarantola, A. [1984]. Inversion of seismic reflection data in the acoustic approximation. *Geophysics*, **49**(8), 1259-1266.

Xu, Wang, Chen, Lambaré and Zhang [2012]. Inversion on reflected seismic wave. SEG Annual Meeting & Exhibition. Expanded Abstract, 1–7.